Geometry, packing, and evolutionary paths to increased multicellular size

Shane Jacobeen, Elyes C. Graba, Colin G. Brandys, Thomas C. Day, William C. Ratcliff, and Peter J. Yunker

Geometry, packing, and evolutionary paths to increased multicellular size

Shane Jacobeen,[1, *] Elyes C. Graba,[1, *] Colin G. Brandys,[1] T.
Cooper Day,[1] William C. Ratcliff,[2] and Peter J. Yunker[1, †]

[1]*School of Physics, Georgia Institute of Technology, North Ave NW, Atlanta, GA 30332*
[2]*School of Biological Sciences, Georgia Institute of Technology, North Ave NW, Atlanta, GA 30332*
(Dated: April 23, 2018)

The evolutionary transition to multicellularity transformed life on earth, heralding the evolution of large, complex organisms. Recent experiments demonstrated that lab-evolved multicellular 'snowflake yeast' readily overcome the physical barriers that limit cluster size by modifying cellular geometry [Jacobeen, et al., Nature Physics, 14 (286-290) 2018]. However, it is unclear why this route to large size is observed, rather than an evolved increase in intercellular bond strength. Here, we use a geometric model of the snowflake yeast growth form to examine the geometric efficiency of increasing size by modifying geometry and bond strength. We find that changing geometry is a far more efficient route to large size than evolving increased intercellular adhesion. In fact, increasing cellular aspect ratio is on average ~ 13 times more effective than increasing bond strength at increasing the number of cells in a cluster. Modifying other geometric parameters, such as the geometric arrangement of mother and daughter cells, also had larger effects on cluster size than increasing bond strength. Simulations reveal that as cells reproduce, internal stress in the cluster increases rapidly; thus, increasing bond strength provides diminishing returns in cluster size. Conversely, as cells become more elongated, cellular packing density within the cluster decreases, which substantially decreases the rate of internal stress accumulation. This suggests that geometrically-imposed physical constraints may have been a key early selective force guiding the emergence of multicellular complexity.

I. INTRODUCTION

The evolution of multicellular organisms from single-celled ancestors set the stage for unprecedented increases in complexity, especially in plants and animals [1, 2]. In nascent multicellular organisms, size and complexity are strongly related [1, 3]; recent work has highlighted the potential for a size-complexity evolutionary feedback loop [2]. However, it is unclear how early, simple multicellular organisms evolved to be larger. Newly multicellular organisms lack genetically-regulated development, growing instead through the stochastic replication of physically-attached individual cells. At high cell densities, stochastic growth can result in large intercellular forces [4], fragmenting groups and limiting multicellular size [5]. Thus, mitigating internal mechanical stress is one of the first evolutionary challenges faced by nascent multicellular organisms. Though the transition to multicellularity occurred independently in at least 25 separate lineages [6, 7], we know little about the physical properties of early multicellular lineages due to their ancient origins and limitations of the fossil record.

Nonetheless, there are two clear routes to increased size in nascent multicellular clusters of cells whose size is limited by the accumulation of internal stress: an organism could evolve to withstand larger intercellular stresses, or, it could evolve to accumulate intercellular stresses at a slower rate during growth. The former strategy would likely involve evolving stronger intercellular bonds,

while the later would involve changes to structural geometry. Geometrically-imposed physical constraints play key roles in the organization of numerous microbial systems, including growing biofilms and swarming or swimming communities [8–11]. Separating geometric effects from biological processes is nontrivial [12], however, and little is known about how simple multicellular systems respond to selection for increased size.

Recently, model systems of simple multicellularity have allowed the early steps of this transition to be studied in the lab with unprecedented precision [13–16]. In the case of 'snowflake yeast' [13], simple multicellular clusters of *Saccharomyces cerevisiae* are subjected to daily selection for large size; they rapidly evolve to double their maximum number of cells per cluster in just seven weeks [5]. Snowflake yeast cluster size is limited by the fracturing of intercellular bonds under growth-induced stresses (Figure 1a). Larger size at fracture is accomplished primarily by a simple change to cluster geometry: over ~ 291 generations, snowflake yeast evolved to have more elongated cells. This increase in cellular aspect ratio decreases the cellular packing fraction, slowing the accumulation of internal stress and delaying fracture [5] (Figure 1b). Cellular elongation is a parallel evolutionary trait, evolving independently in replicate populations [5, 17]. However, it remains unclear *why* this evolutionary route to large size is repeatedly observed: do snowflake yeast clusters modify geometry because it is more effective than increasing the strength of cell-cell bonds, or for proximate reasons relating to the model system (e.g., it may be easier to modify geometry than bond strength)?

To investigate the roles of geometry and bond strength in the evolution of nascent multicellularity, we employ

a geometric model of experimentally-evolved snowflake yeast [13, 17, 18], introduced and experimentally validated in Jacobeen *et. al.*, 2018 [5]. We find that modifying packing geometry, and thus slowing the accumulation of internal stresses, is a far more efficient route to large size than increasing intercellular bond strength. This result is likely general, as cells are capable of imparting tremendous forces during growth [4], and the resulting cell-cell forces increase rapidly in jammed aggregates. Thus, evolving physical robustness by modifying multicellular geometry may have been a key early selective force guiding the emergence of multicellular complexity.

II. BACKGROUND

We simulate the growth of snowflake yeast clusters with a simple, three-dimensional geometric model [5] based on their fractal-like growth pattern [13]. The model is purely structural, *i.e.*, it lacks dynamics, yet it accurately reproduces many relevant experimentally-measured structural properties of snowflake yeast [5] (for more details on experimental validation of the model, please see the Supplemental Information).

A. Model

Snowflake yeast cells reproduce via budding [13]; daughter cells remain attached to their mothers, creating a biologically and physically tractable multicellular cluster (Fig. 1a). In our simulation, cells are modeled as prolate spheroids (ellipsoids in which two 'equatorial' radii are equal and less than the polar radius), with major-minor axis aspect ratio α. Each generation, all cells in the cluster attempt to reproduce by adding a daughter cell of identical volume on their surface. Daughter cells are placed at a specified angle from the polar axis, called the angle of attachment, θ, where θ is the acute angle between the parent cell's major axis and a vector that originates at the geometric center of the cell and passes through the point on its surface at which the daughter cell attaches (Fig. 1c). Thus, daughter cells are randomly placed along a 'budding ring' on their parent's surface (Fig. 1d). Additionally, cells other than the basal cell have an 80% chance of spawning at the pole opposite their parent (that is, with $\theta = 0$) on their initial reproduction attempt. Cellular bodies may overlap (Fig. 1e), but the center-to-center separation may not be less than 50% of their small diameter; this constraint is analogous to disallowing the overlap of bud scars (*i.e.*, attachment sites). If the randomly selected attachment site would cause too much (>50%) overlap, the daughter cell is not created and the parent cell misses their chance to reproduce that generation.

Varying θ and α facilitate changes to cluster geometry. To vary bond strength, we first calculate the deformation energy (u) between the bodies of neighboring cells. That
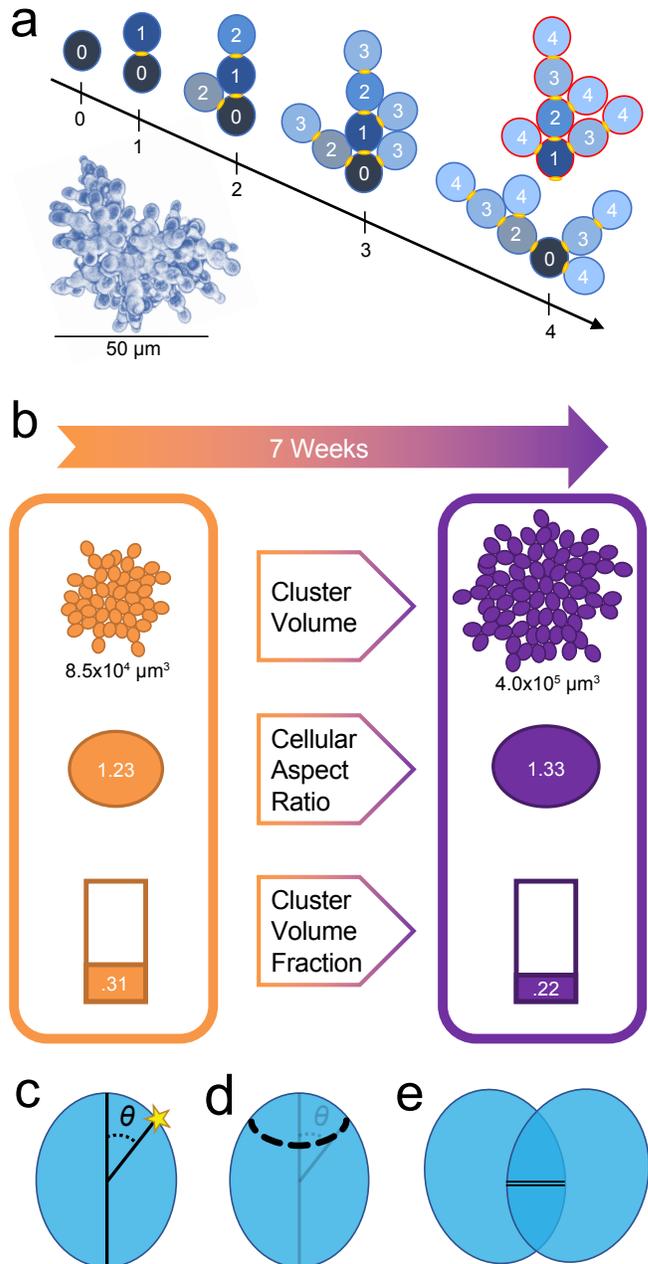

FIG. 1. (a) 2D schematic of snowflake yeast growth morphology, showing fracture due to cellular crowding. Inset: 3D confocal image of a snowflake yeast cluster. (b) Changes over 7 weeks of experimental evolution in mean values of snowflake yeast cluster size, cellular aspect ratio, and cluster volume fraction. (c-e) describe the geometric simulation of cluster growth; (c) new cells are added on the surface of their parent at an attachment site (yellow star) defined by the polar angle θ from the major axis of the cell; this angle is referred to as the 'angle of attachment'. (d) Rotating θ around the major axis of the cell defines a ring on its surface along which daughter cells may be randomly placed (dashed line); this ring is termed the 'budding ring'. (e) The length of the double line illustrates the linear overlap between two cells.

is

$$u_{ij} = (d - r_i - r_j)^2 \qquad (1)$$

where d is the center-to-center distance between overlapping cells, and r_i and r_j are the equatorial radii of two neighboring cells. $u_{ij} = 0$ for non-overlapping cells, and the total 'deformation energy' (U) in a cluster is the sum of individual u_{ij}:

$$U = \sum_{i=1}^{N} \sum_{j \neq i}^{N} u_{ij} \qquad (2)$$

where N is the number of cells in the cluster. In a real cluster, cells would bend at their cell-cell bonds rather than overlap, so linear overlap acts as a proxy for deformation and squared overlap is a proxy for deformation energy, or internal stress within the cluster (using a Hertzian, rather than a harmonic model for deformation energy does not qualitatively change the results of this simulation [5]). As clusters fracture due to an asymmetric accumulation of internal stress concentrated in the core of the cluster [5] (Fig S1d), we use a U threshold (U_c) to limit cluster size. Snowflake clusters fracture when their internal stress exceeds the ultimate strength of the cell-cell bonds; thus, changing U_c is analogous to changing bond strength.

As previously reported in Jacobeen *et. al.*, 2018 [5], this geometric model recapitulates many key structural features observed in experiments. Experimentally evolved isolates were modeled by randomly picking each new cell's α from experimentally measured distributions. These simulations revealed that as mean cellular α increases, cluster volume fraction decreases. In fact, simulations closely replicate experimental observations: simulated and experimentally measured packing fractions are within 5% of each other for all four genotypes studied (the validation of the model via comparison with experimental results is detailed in [5] and in the Supplemental Information here). As internal stress limits cluster size by fracturing intercellular bonds, the decrease in volume fraction due to cellular geometry modification likely plays a large role in the evolved increase in cluster volume over seven weeks [5] (Figure 1b).

III. RESULTS

To directly compare the efficiency of increasing cluster size via cellular elongation and increased bond strength, we first simulated clusters with a wide range of α and U_c values (we set $\theta = 54°$, as cluster size is maximized for this value). We varied α and U_c between 1.0 and 2.0 in steps of 0.1, and simulated 100 clusters for each pair of parameters (Fig. 2a). The mean number of cells per cluster increases rapidly with increasing α for any value of U_c (Fig. 2a and b). In contrast, the mean

number of cells increases much more slowly with increasing U_c (Figure 2a and c). Thus increasing α is a more efficient path to large size than increasing U_c.

While increasing α always increases cluster size more then increasing U_c, the size of this disparity varies. For example, the smaller α is, the more beneficial it is to increase α than U_c. In fact, for clusters of spherical cells ($\alpha = 1.0$), it is on average ~ 59 times more effective to increase α than to increase U_c (*i.e.*, for small α, there is almost no discernible gradient along the U_c axis (Fig. 2a)). Thus, there is an especially large incentive to increase aspect ratio at least a little above 1.0. Further, increasing U_c always enlarges the incentive for increasing α; this is visible in Fig. 2a as the strength of the vertical gradient increases with U_c. Though the relative superiority of increasing α over U_c varies over the studied range of parameters – generally decreasing significantly with increasing α and increasing with U_c – it is always at least 2.5 times more effective to increase α, and on average ~ 13 times more cells are added for an increase of .1 in α than for an increase of the same magnitude in U_c.

Why is increasing aspect ratio a more efficient route to large size than increasing bond strength? To investigate, we measured the deformation energy in simulated clusters as a function of the mean number of cells. U increases $\sim$quadratically with N for any value of α (Figure 3a). Thus, increasing U_c yields sub-linear returns ($N \sim \sqrt{U_c}$). However, increasing α causes U to increase at a slower rate, allowing more cells to be added before U_c is reached. The linear relationship between N and α (Fig. 2c) further demonstrates the superior returns on increasing α rather than U_c.

To understand how cellular aspect ratio affects internal stress accumulation, we calculated the linear packing fraction (*i.e.*, the occupied fraction of the budding ring) of 5 non-overlapping daughter cells on a parent cell for $\theta = 54°$ (5 cells was chosen because it is the maximum number that can be placed at $\theta = 54°$ for all values of α between 1 and 2) (Figure 3b). Considering that daughter cells maximize their available space when they are oriented perpendicular to the long axis of their parent, linear packing fraction ϕ, is

$$\phi = \frac{n \cdot 2 \cdot r_{min}}{2 \cdot \pi \cdot (r_\theta + \alpha \cdot r_{min})} \qquad (3)$$

where n is the number of daughter cells, r_{min} is the minor radius, and r_θ is the radius at θ. Larger α daughter cells have smaller widths; smaller widths make it less likely for any two cells to overlap. Thus, more cells must be added to clusters with large α to obtain the same packing fraction - and U - as clusters with small α.

We also investigated other geometric parameters, to determine if the effects of α represented an isolated case. We varied θ between 30° and 90° in increments of 12° and again varied U_c from 1.0 to 2.0 in steps of 0.1. For each pair of parameters, 100 independent simulations
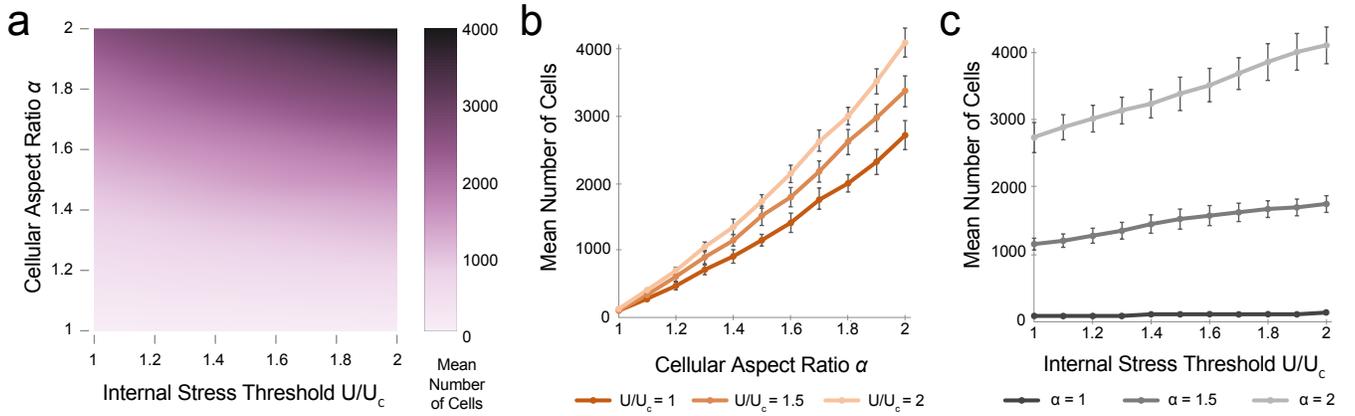
FIG. 2. (a) Interpolated heat map of the mean number of cells in a cluster as a function of cellular aspect ratio (α) and deformation energy threshold (U_c). (b) Mean number of cells per cluster versus α for U_c (dark orange, bottom), $1.5U_c$ (medium orange, middle), and $2U_c$ (light orange, top). (c) Mean number of cells per cluster versus U_c for $\alpha = 1.0$ (dark gray, bottom), $\alpha = 1.5$ (medium gray, middle), and $\alpha = 2.0$ (light gray, top). Each data point is the average of 100 independent simulations. Error bars indicate standard deviation.
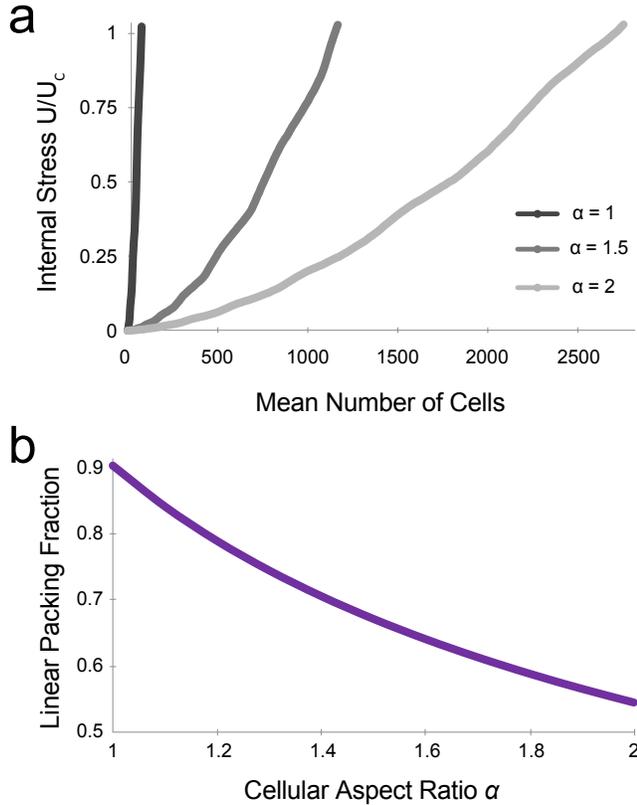

FIG. 3. (a) As a cluster grows, total deformation energy, U, increases as well. This increase is rapid when $\alpha = 1$ (dark gray, left), moderate for $\alpha = 1.5$ (medium gray, middle), and slowest for $\alpha = 2$ (light gray, right). Each overlapping data point is the average of 100 independent simulations. (b) Linear packing fraction for 5 daughter cells on a single mother cell as a function of aspect ratio for $\theta = 54°$.

were conducted with $\alpha = 1.5$, and the resulting mean

values are shown in the interpolated heat map in figure 4a. As previously mentioned, cluster size is maximized when $\theta = 54°$ for all values of U_c (note, $\theta = 54°$ is within the experimentally observed range [5]). This is due to a trade-off between local and global packing effects. The number of cells that can pack on a single parent increases with θ–up to $\theta = 90°$–because the circumference around which daughters are packed is largest at $\theta = 90°$. However, branches within a cluster interfere with each other less for smaller values of θ; $54°$ is the angle where the trade-off between these competing affects is maximized. Additionally, changing θ (moving it closer to $\theta = 54°$) is generally a more efficient route to increase cluster size than increasing U_c, especially if θ is far from $\theta = 54°$. However, since an optimal value of θ exists (unlike with α), when θ is close to $54°$, increasing U_c is more beneficial. Note, the optimum angle is near the so-called 'magic angle', $\theta = 54.7°$[19], suggesting that the snowflake yeast structure is analogous to packing cells in cones (see SI for more details).

Finally, we investigated the effect of heterogeneity in geometric parameters. Along with providing another geometric parameter to check, monodisperse values of α and θ are biologically unrealistic, as real snowflake yeast clusters feature polydispersity in both parameters [5]. First, a single pair of α and θ parameters was chosen; we selected $\alpha = 1.5$ because it is in the center of the range of values studied and is within the experimentally observed range, and $\theta = 54°$ because it is the optimum value of θ. Variance is introduced in the form of a truncated Gaussian distribution centered on each selected parameter. For every cell added, the value of each parameter is chosen from a self-centered Gaussian distribution; however, if the value selected lies outside the relevant range (1.0 - 2.0 for α, $30°$ to $90°$ for θ), another value is randomly selected. We simulated 100 independent clusters for Gaussians with standard deviations of 0.05, 0.10, and

0.20 of the mean θ or α.

We find that variance in both α and θ has little effect on cluster size when it is relatively small (standard deviation / mean ≤ 0.1); larger variances, however, (> 0.1) decrease cluster size (Figure 4b). The inverse relationship between size and large variance is expected for θ; any deviation from the optimal value naturally leads to smaller clusters. However, the relationship between N and *alpha* is highly linear (figure 2b), meaning that the detriments of smaller aspect ratio cells must outweigh the benefits of longer aspect ratio cells within these disordered clusters. If the standard deviation in alpha decreases from 0.2 to 0.1, the resulting increase in cluster size is the same as that caused by an increase in α of $\sim .04$ or and increase in U_c of $\sim .26$, again supporting the idea that modifying geometry provides a larger return to the cluster size than modifying bond strength.
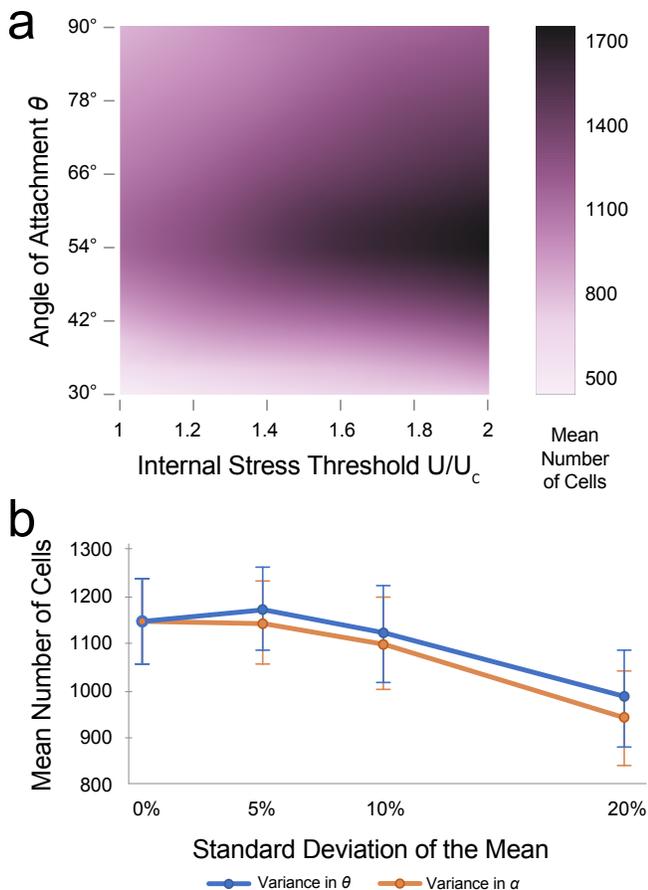

FIG. 4. (a) Interpolated heat map of the mean number of cells in a cluster as a function of angle of attachment (θ) and deformation energy threshold (U_c). (b) Effect of variance in the angle of attachment(θ) and cellular aspect ratio(α) on cluster size. The number of cells in a cluster versus the standard deviation of the truncated Gaussian distribution for θ (blue, upper) and α (orange, lower). Each data point is the average of 100 independent simulations. Error bars indicate standard deviation.

IV.   DISCUSSION

Evolutionary benefits stemming from size are thought to be a key driver of early multicellularity [2, 6], affording protection from common threats to microbial life (*e.g.*, predation and toxin exposure [20–22]). However, *how* large physical size could be achieved by newly multicellular organisms has remained poorly understood. Recent work revealed that snowflake yeast evolve increased size via modifications to cellular geometry[5]; here, we offer evidence for *why* this route was observed. Geometric modeling reveals that modifying geometry – via three different parameters – is a significantly more effective means to achieve larger cluster size than increasing bond strength. Internal stress increases rapidly with cellular reproduction, so investing in bond strength produces diminishing returns. Conversely, modifying cell shape, budding angle, or the variance of these quantities changes how cells pack, slowing the accumulation of internal stress.

Our results highlight the absolute limit of spatial constraints. Two cells cannot overlap, so at high cell density the addition of new cells rapidly increases internal stress. The optimal strategy is not to increase bond strength in the face of vanishing free space, but to pack more efficiently so free space remains available longer. The rapid increase in internal stress with increasing cell number is reminiscent of the jamming transition of athermal grains, for which pressure increases with increasing packing fraction [23, 24]. Previously reported experiments on unicellular yeast demonstrated that reproduction in dense cellular packings can exert pressures on the order of 1 MPa [25]. Thus, a $\sim 3\mu m$ diameter bud scar may experience forces on the order of 10 μN. This is orders of magnitude larger than the ~ 100 pN force necessary to break mammalian intercellular bonds [26, 27] or tear bacteria from a biofilm [28]. Thus, resisting forces from growth at high cell density would require major innovations on known intercellular adhesion mechanisms.

While snowflake yeast is a lab-evolved model system, it possesses a number of features generally agreed to be common to naturally occurring nascent multicellular organisms. Snowflakes develop clonally, growing through mother-daughter cell adhesion with regular genetic bottlenecks[13, 18]. This facilitates multicellular adaptation, as it limits the potential for within-organism genetic conflict and promotes the emergence of novel, heritable multicellular traits [29]. Snowflake yeast readily adapt as multicelluarity individuals, evolving to be more complex by gaining novel multicellular traits [13, 17, 30]. Indeed, complex multicelluarity (*i.e.*, metazoans, land plants, red algae, brown algae and fungi) has only evolved in organisms that develop clonally[31]. Our geometric arguments are easily generalized to other organisms with fixed-geometry morphology. Interestingly, this appears

to be the dominant path to complexity: all independent transitions to complex multicellularity, with the exception of animals, grow with rigidly connected cells in a fixed-geometry body plan. Taken together, our results demonstrate that biophysical interactions play a critical role in the evolutionary transition to multicellularity.

[1] D. L. Kirk, BioEssays **27**, 299 (2005).

[2] A. H. Knoll, Annual Review of Earth and Planetary Sciences **39**, 217 (2011).

[3] M. Willensdorfer, Journal of evolutionary biology **21**, 104 (2008).

[4] M. Delarue, J. Hartung, C. Schreck, P. Gniewek, L. Hu, S. Herminghaus, and O. Hallatschek, Nature physics **12**, 762 (2016).

[5] S. Jacobeen, J. T. Pentz, E. C. Graba, C. G. Brandys, W. C. Ratcliff, and P. J. Yunker, Nature Physics **14**, 268 (2018).

[6] J. T. Bonner, Integrative Biology: Issues, News, and Reviews **1**, 27 (1998).

[7] R. K. Grosberg and R. R. Strathmann, Annual Review of Ecology, Evolution, and Systematics **38**, 621 (2007), https://doi.org/10.1146/annurev.ecolsys.36.102403.114735.

[8] W. P. J. Smith, Y. Davit, J. M. Osborne, W. Kim, K. R. Foster, and J. M. Pitt-Francis, Proceedings of the National Academy of Sciences (2016), 10.1073/pnas.1613007114.

[9] B. Ilkanaiv, D. B. Kearns, G. Ariel, and A. Beer, Physical Review Letters **118** (2017), https://doi.org/10.1103/PhysRevLett.118.158002.

[10] O. Guadayol, K. L. Thornton, and S. Humphries, Scientific Reports **7** (2017), 10.1038/s41598-017-01565-y.

[11] J. Varennes, S. Fancher, B. Han, and A. Mugler, Phys. Rev. Lett. **119**, 188101 (2017).

[12] D. T. Fraebel, H. Mickalide, D. Schnitkey, J. Merritt, T. E. Kuhlman, and S. Kuehn, eLife **6**, e24669 (2017).

[13] W. C. Ratcliff, R. F. Denison, M. Borrello, and M. Travisano, Proceedings of the National Academy of Sciences **109**, 201115323 (2012).

[14] M. D. Herron, J. D. Hackett, F. O. Aylward, and R. E. Michod, Proceedings of the National Academy of Sciences of the United States of America **106**, 3254 (2009).

[15] J. H. Koschwanez, K. R. Foster, and A. W. Murray, eLife **2**, e00367 (2013).

[16] W. C. Ratcliff, M. D. Herron, K. Howell, J. T. Pentz, F. Rosenzweig, and M. Travisano, Nature Communications **4** (2013).

[17] W. C. Ratcliff, J. T. Pentz, and M. Travisano, Evolution **67**, 1573 (2013).

[18] W. C. Ratcliff, J. D. Fankhauser, D. W. Rogers, D. Greig, and M. Travisano, Nature Communications **6**, 6102+ (2015).

[19] S. J. Erickson, R. W. Prost, and M. E. Timins, Radiology **188**, 23 (1993), pMID: 7685531, https://doi.org/10.1148/radiology.188.1.7685531.

[20] S. Smukalla, M. Caldara, N. Pochet, A. Beauvais, S. Guadagnini, C. Yan, M. D. Vinces, A. Jansen, M. C. Prevost, J.-P. Latgé, G. R. Fink, K. R. Foster, and K. J. Verstrepen, *Cell*, Cell **135**, 726 (2008).

[21] M. E. Boraas, D. B. Seale, and J. E. Boxhorn, Evolutionary Ecology **12**, 153 (1998).

[22] R. H. Kessin, G. G. Gundersen, V. Zaydfudim, and M. Grimson, Proceedings of the National Academy of Sciences **93**, 4857 (1996), http://www.pnas.org/content/93/10/4857.full.pdf.

[23] A. J. Liu and S. R. Nagel, Annual Review of Condensed Matter Physics **1**, 347 (2010), https://doi.org/10.1146/annurev-conmatphys-070909-104045.

[24] H. M. Jaeger, S. R. Nagel, and R. P. Behringer, Rev. Mod. Phys. **68**, 1259 (1996).

[25] M. Delarue, J. Hartung, C. Schreck, P. Gniewek, L. Hu, S. Herminghaus, and O. Hallatschek, Nature Physics **12**, 762 EP (2016).

[26] Y. Hosokawa, M. Hagiyama, T. Iino, Y. Murakami, and A. Ito, Proceedings of the National Academy of Sciences **108**, 1777 (2011), http://www.pnas.org/content/108/5/1777.full.pdf.

[27] S. Bajpai, Y. Feng, R. Krishnamurthy, G. D. Longmore, and D. Wirtz, The Journal of Biological Chemistry **284**, 18252 (2009).

[28] Y. Hu, J. Ulstrup, and J. Zhang, *Bacterial biofilms investigated by atomic force microscopy and electrochemistry*, Ph.D. thesis (2012).

[29] W. C. Ratcliff, M. Herron, P. L. Conlin, and E. Libby, Phil. Trans. R. Soc. B **372**, 20160420 (2017).

[30] J. T. Pentz, B. P. Taylor, and W. C. Ratcliff, Journal of The Royal Society Interface **13**, 20160121 (2016).

[31] T. Brunet and N. King, Developmental cell **43**, 124 (2017).